ELSEVIER

Journal of Nuclear Materials 270 (1999) 253–258

journal of nuclear materials

Uranium dioxide reaction in CF_4/O_2 RF plasma

Yong-soo Kim [a,*], Jin-young Min [a], Ki-kwang Bae [b], Myung-seung Yang [b]

[a] *Department of Nuclear Engineering, Hanyang University, 17 Haengdang-Dong, Sungdong-Ku, Seoul 133-791, South Korea*
[b] *Korea Atomic Energy Research Institute, P.O. Box 7, Taejon 305-606, South Korea*

Received 7 May 1998; accepted 19 October 1998

Abstract

Research on the fluorination reaction of UO_2 in CF_4/O_2 RF plasma is carried out at temperatures of up to 370°C under total pressure of 0.3 Torr. The reaction rates are investigated as functions of CF_4/O_2 ratio, plasma power, substrate temperature, and exposure time to the plasma. It is found that there exists an optimum CF_4/O_2 ratio of around four for the efficient etching, regardless of RF power and substrate temperature. According to the mass spectrometry it is revealed that the major reaction product is uranium hexa-fluoride UF_6. Some minor species such as UF_4 and UF_5 are probably generated parasitically. The highest etching reaction rate at 370°C under 150 W exceeds 1000 monolayers/min, which is equivalent to 0.4 μm/min. Based on the experimental findings, dominant overall reaction of uranium dioxide in CF_4/O_2 plasma is determined: $UO_2 + 3/2\,CF_4 + 3/8\,O_2 = UF_6 + 3/2\,CO_{2-x}$, where CO_{2-x} represents the undetermined mix of CO_2 and CO. The overall reaction follows a linear kinetics and is thus rate-determined by the surface reaction between the uranium atom in UO_2F_2 intermediates on the surface and incoming fluorine atoms or fluorine containing radicals. The activation energy of this reaction is derived as 12.1 kJ/mol.

1. Introduction

The fluorination of uranium dioxide has been extensively studied in the application-oriented fields such as uranium separation, processing, and conversion [1–4]. Along with the applied research, fundamental studies of the UO_2/F_2 reaction have been reported by several authors [5–10].

The reaction of UO_2 at low temperatures of below 800 K under atmospheric pressure of F_2 was studied using weight loss measurements by Vandenbussche [6] and Iwasaki [7]. Under these conditions the ultimate reaction products are found to be UF_6 and O_2, while a variety of intermediate reaction products such as $(UO_2)_4F$ and UO_2F_2 are identified. On the contrary, a quasi-equilibrium reaction modelling study predicted that at high temperatures of above 1000 K under low pressure of F_2 ($10^{-7} \sim 10^{-4}$ Torr), uranium hexa- and penta-fluoride formations are suppressed in favor of UF_4 and atomic fluorine formation [8,9]. A kinetic study carried out later at high temperatures of above 1000 K under ultra-high vacuum condition confirmed that the reaction product is UF_4 and the reaction probability is about 10^{-2} [10]. The authors claimed that the reaction mechanism is a second-order surface reaction coupled with the double-diffusion process.

The disagreement between these early experimental results seems to stem from the different ranges of temperatures and pressures. Thus, the extrapolation of the results in one range to another must be carefully made even in cases of necessity.

Recently the feasibility of burning spent PWR fuel in a CANDU reactor was carried out, in which decladding of spent fuel pins and dry-processing of burned uranium dioxide such as OREOX (Oxidation and REduction of OXide fuel) process are the main processes to make re-sinterable fuel powder [11,12]. In the process, however, most candidate decladding techniques were unable to recover more than 98%–99.5% of the heavy metal/metal oxide. A part of the remainder will be present as adherent dust and some may also be

---

[*] Corresponding author: Tel.: +82-22 290 0467; fax: +82-22 281 5131; e-mail: yongskim@numater.hanyang.ac.kr

0022-3115/99/$ – see front matter © 1999 Elsevier Science B.V. All rights reserved.
PII: S0022-3115(98)00906-4

chemically bonded to the zirconium oxide layer on the inside of the fuel pin. Therefore, another process for additional removal of the last portion of the fuel is required, which also removes alpha contamination from the clad to a level qualifying the fuel hulls as non-TRU. For the secondary decontamination process, a plasma processing technique using fluorine containing gas plasma was proposed and its applicability has been demonstrated [13].

Following the demonstration, the reaction rates of uranium dioxide in CF_4/O_2 plasma and overall reaction mechanism is investigated in detail in this paper to provide the basics for the future eventual application of the technique to irradiated fuel materials.

2. Experimental

The apparatus for the etching reaction in CF_4/O_2 mixture gas plasma is designed and manufactured to meet the experimental purposes (Fig. 1). The plasma reactor is a diode type and RF power of up to 600 W is applied between the parallel electrodes. The distance between them can be adjusted from 4 cm up to 12 cm. However, it remained stationary (10 cm) during the current experiments. The heating element in the reaction chamber can heat samples, mostly thin disk or wafer-like samples of maximum 10 cm diam, up to 800°C. Total gas pressure is varied using the main throttle valve and O_2 mole fraction is fine-controlled with mass flow controllers.

In the experiments thin disks (0.35 mm in thickness) of natural uranium dioxide cut out of a pellet are used as specimens. Total gas pressure is maintained at 0.3 Torr and RF plasma power of up to only 150 W is applied because of temperature control difficulties resulting from internal heating of the chamber.

Prior to the sample loading, specimens are polished by grit 600 sandpaper, cleaned by ultrasonic cleaner, and baked at 200°C for 10 min in a ultra-high vacuum to evaporate the adsorbed moisture on the surface.

Reactants and generation of reaction products are in situ detected and identified by a PC-controlled quadrupole mass spectrometer (model HAL-3F/PIC, Hiden Anal. Ltd.) sitting in the detection chamber. The probe comprises a quadrupole mass analyzer, on which is mounted an electron bombardment source to create ions from the neutral molecules, and a detector to measure the ion current.

Etching reaction rate is determined by weight loss measurement before and after the reaction with an electro-micro balance (BP210D, Sartorius) whose sensitivity limit is 10^{-5} g.

3. Results and discussion

First, under RF power of 100 W and 150 W, etching reactions are examined with various CF_4/O_2 ratios for 100 min at several substrate temperatures of up to 370°C. The etching rate is estimated using the following formula

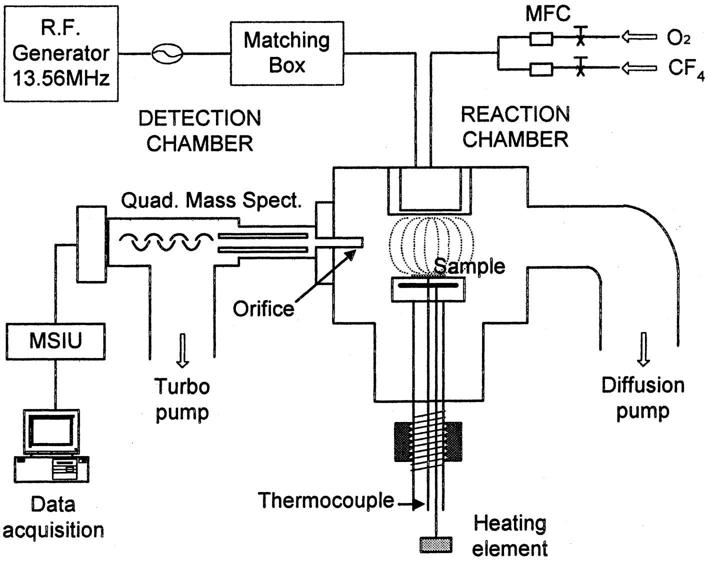

Fig. 1. A schematic of plasma etching reaction apparatus

$$\frac{1}{(\rho\ N_a/M)^{2/3}}\frac{\Delta W}{At}\frac{N_a}{M}\quad \text{(monolayers/min)},$$

where ρ is UO_2 density (10.96 g/cm^3), N_a is Avogadro's number, M is UO_2 atomic mass (270.03 g/mole), ΔW is weight loss due to etching reaction, A is area of the sample, and t is duration of exposure to plasma.

The experimental results are plotted in Fig. 2(a) and (b). The figures reveal that there exists an optimum CF_4/O_2 ratio for the efficient etching of UO_2, regardless of RF power and substrate temperature, and that it is around 4 under the substrate temperature of 370°C. It is also found that the etching reaction rate at the optimum gas composition increases as substrate temperature and/or RF plasma power go up.

The highest etching reaction rate at 370°C under 150 W exceeds 1000 monolayers/min, which is equivalent to 0.4 μm/min and comparable to that of the Si wafer in the semi-conductor industry.

Reactants and reaction products are in situ identified by the quadrupole mass spectrometer in the detection chamber. Typical examples of detected species over the mass spectrum are shown in Fig. 3(a) and (b). The first figure shows that a lot of stable or meta-stable compounds containing fluorine such as COF_2, COF, F_2 and F are produced in CF_4/O_2 plasma, which is in good agreement to the previous results [14]. From the elementary reaction point of view, therefore, the molecular and/or atomic fluorine produced in the plasma or dissociated from the intermediate species are believed to take part in the fluorination reaction of uranium dioxide. In fact, CF_4/O_2 is one of the most popular gas mixtures used for fluorination of silicon in the semiconductor industry [15,16]. It is also used for TRU decontamination such as plutonium [17]. As a result of its popularity, a number of studies on the gas phase reaction of the mixture plasma have been carried out [15–17].

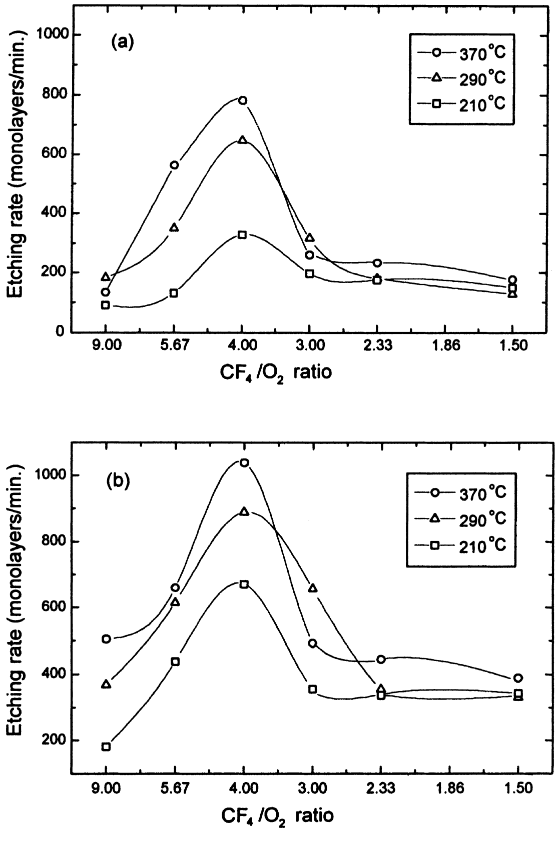

Fig. 2. Etching reaction rate vs. O_2 mole fraction (a) 100 W RF plasma; (b) 150 W RF plasma

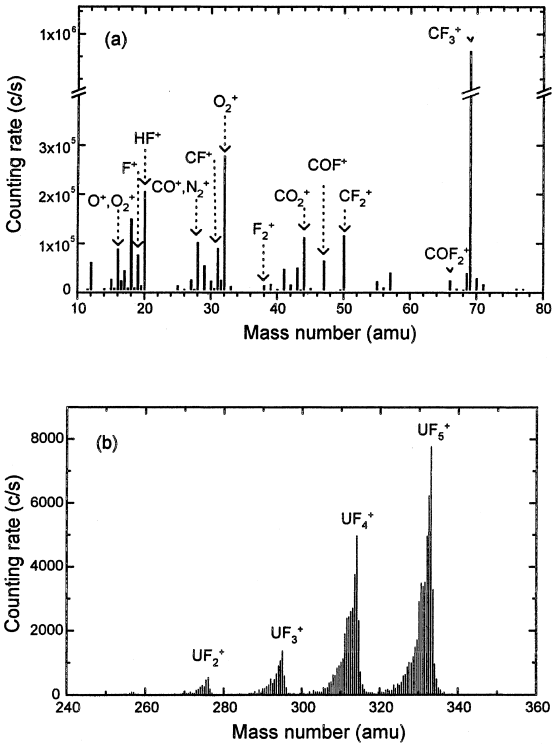

Fig. 3. (a) Reactants discharged in CF_4/O_2 plasma and (b) reaction products of UO_2 in CF_4/O_2 plasma

As expected, Fig. 3(b) reveals that several uranium fluorides are produced in the reaction, and apparently, UF_5 seems to be the most abundant species among the reaction products. However, according to the thermodynamic instability of UF_5 and characteristic fragmentation pattern of UF_6 (0.004 UF_6^+, 1.00 UF_5^+, 0.262 UF_4^+, 0.283 UF_3^+, 0.332 UF_2^+ [18]), it is concluded that the major reaction product is uranium hexa-fluoride, UF_6, and the minor species such as UF_4 and UF_5 are probably generated parasitically.

Based on the finding that there exists an optimum gas composition in this fluorination reaction and that the major reaction product is UF_6, the dominant overall reaction of uranium dioxide in CF_4/O_2 plasma is determined:

$$UO_2 + 3/2CF_4 + 3/8O_2 = UF_6 + 3/2CO_{2-x},$$

where CO_{2-x} represents the undetermined mix of CO_2 and CO.

In the fluorination of UO_2 to UF_6 with fluorine, the formation of UO_2F_2 on the surface as a primary intermediate has already been reported [5,19]. For the identificaton of this species, the surface elements of reacted and unreacted specimens are analyzed by XPS (X-ray photoelectron spectroscopy) in Fig. 4.

The fluorine peak re-plotted in detail in Fig. 5(a) shows that the intact UO_2 specimen has no fluorine on the surface while the reacted surface is covered with the compounds of uranium, oxygen, and fluorine. This confirms that fluorine compounds, possibly UO_2F_2, form on the surface during the reaction. The peaks of constituent elements over a binding energy spectrum referenced to binding energy of O_{1s} in UO_2 are examined. In fact, binding energies of both $U_{4f7/2}$ and $U_{4f5/2}$ in the reacted specimen closely fall in with those of the two U peaks in UO_2F_2, which are shifted up by 2.9 eV from those of intact UO_2 [20].

Carbon peaks are also re-plotted in detail in Fig. 5(b). During the experiment, oxygen gas is injected in the feed gas to pick up and remove the carbon atoms by forming volatile species such CO or CO_2, since carbon residuals decomposed from carbon tetra-fluoride may deposit on the surface and suppress surface reaction. Thus, it is supposed that at oxygen gas compositions of lower than the optimum, the amount of oxygen (molecule or atom) is not enough to pick up the carbon residuals. Hence, the surface carbon concentration is greater than that of the optimally reacted surface. This claim is supported by XPS analysis in the figure showing that the concentration is much lower than that of the non-optimum composition (10% O_2).

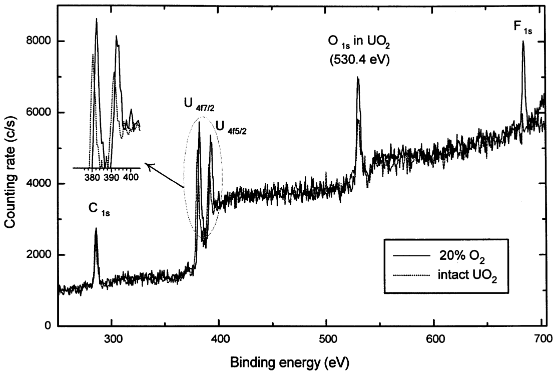

Fig. 4. XPS spectrum of UO_2 specimen before and after reaction. (Binding energy of O_{1s} in UO_2 is used as a reference.)

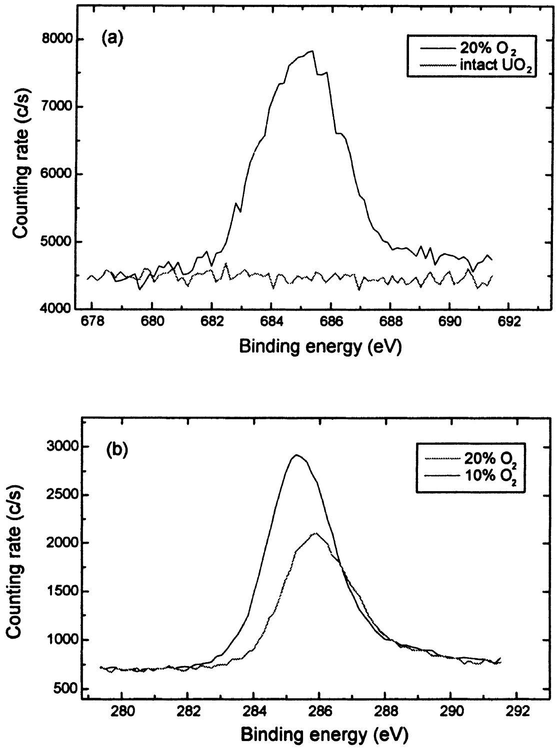

Fig. 5. (a) Fluorine peak in detail; (b) carbon peak in detail in Fig. 4

At higher oxygen gas compositions, on the other hand, high reactivity of excessive oxygen with surface uranium atom may form hyper-stoichiometric uranium oxides instead of forming CO or CO_2 and interfere with the formation of volatile uranium fluorides. This postulation is demonstrated by XRD (X-ray diffractometry) analysis in Fig. 6. In the figure, stronger peaks of uranium compounds such as U_4O_9, U_3O_7, and U_3O_8 are more clearly seen in the uranium dioxide reacted in $40\%O_2/60\%CF_4$ plasma than those reacted in $20\%O_2/80\%CF_4$ plasma.

Fig. 7 shows the weight loss of the UO_2 disk with reaction time at several temperatures from 210°C–370°C. Incubation period is not observed in the results unlike in earlier works, and the reaction kinetics follows a linear rate law.

In general, in the fluorination reaction of uranium dioxide, the following consecutive process is considered as a simplified model

$$UO_2 \rightarrow UO_2F_2 \rightarrow UF_6.$$

While the first step of the process must involve the diffusion of the fluorine atom on the surface and/or into the matrix, the second step is a simple surface reaction. Nevertheless, Fig. 7 demonstrates that the overall reaction follows a linear kinetics, that is, surface-reaction

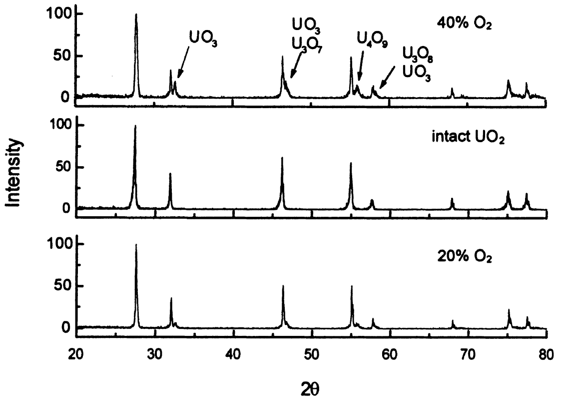

Fig. 6. XRD patterns of UO_2 specimen before and after reaction

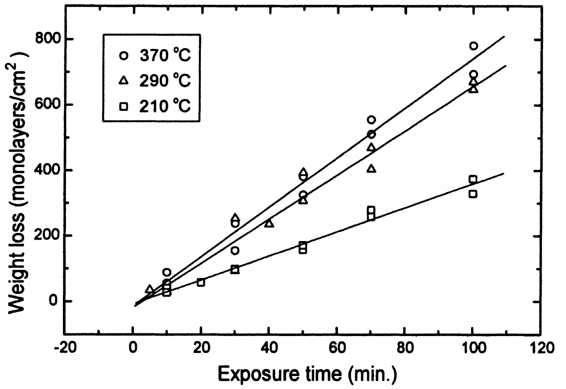

Fig. 7. Weight loss vs. exposure time in $80\%CF_4/20\%O_2$ plasma

rate-limiting. This means that the second part of the process governs the reaction between the uranium atom in UO_2F_2 intermediates on the surface and incoming fluorine atoms or fluorine containing radicals in the CF_4/O_2 plasma. This may be primarily because the temperature range in the current study is not high enough for the fluorine atom to diffuse vigorously, therefore, first step does not contribute much in the overall reaction.

Based on the linear kinetics, activation energy of the reaction is derived as 12.1 kJ/mol in Fig. 8 and this is comparable to 10.4 kJ/mol for Si and 15.8 kJ/mol for SiO_2 [17,21]. Compared to earlier fluorination works of UO_2 [7,10], it is quite low because they were carried out at very high temperatures of above 1000 K or at mid-temperatures of around 300°C–540°C under atmospheric pressure in which fluorine atom diffusion and UO_2F_2 formation reaction are deeply involved. It must be taken into consideration that this fluorination reaction of UO_2 in CF_4/O_2 plasma is a kind of catalytic reaction.

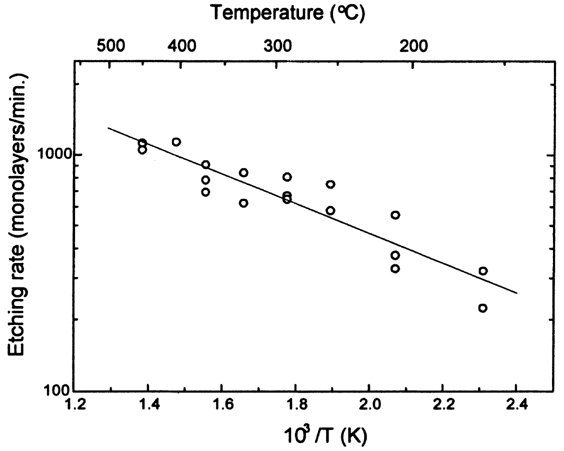

Fig. 8. Etching reaction rate vs. substrate temperature in $80\%CF_4/20\%O_2$ plasma

4. Conclusions

From the current investigation it is found that there exists an optimum CF_4/O_2 ratio for the efficient etching of UO_2 in CF_4/O_2 plasma, regardless of RF power and substrate temperature. The ratio is around 4 under the substrate temperature of 370°C. This optimum gas composition is explained by the following experimental findings: at oxygen gas compositions of lower than the optimum, the amount of oxygen is not enough to pick up the carbon residuals, hence, the residuals decomposed from carbon tetra-fluoride may deposit on the surface and suppress surface reaction, on the other hand, at higher oxygen gas compositions, high reactivity of excessive oxygen with surface uranium atoms may form hyper-stoichiometric uranium oxides instead of carbon mono- or dioxide and interfere with the formation of volatile uranium fluorides.

The highest etching reaction rate at 370°C under 150 W exceeds 1000 monolayers/min, which is equivalent to 0.4 μm/min and comparable to that of the Si wafer in the semi-conductor industry.

According to the mass spectrometry, it is revealed that the major reaction product is uranium hexa-fluoride UF_6. Some minor species such as UF_4 and UF_5 are probably generated parasitically. Therefore, based on the experimental results the dominant overall reaction of uranium dioxide in CF_4/O_2 plasma is determined

$$UO_2 + 3/2CF_4 + 3/8O_2 = UF_6 + 3/2CO_{2-x},$$

where CO_{2-x} represents the undetermined mix of CO_2 and CO.

XPS analysis confirms that UO_2F_2 compound forms on the surface during the reaction as a primary intermediate and additional experiments show that reaction kinetics follows a linear rate law.

Therefore, it is concluded that the overall reaction of this fluorination of uranium dioxide in CF_4/O_2 plasma is rate-determined by the surface reaction between the uranium atoms in UO_2F_2 intermediates on the surface and incoming fluorine atoms or fluorine containing radicals. The activation energy of this reaction is derived as 12.1 kJ/mol, which is comparable to 10.4 kJ/mol for Si and 15.8 kJ/mol for SiO_2.

References

[1] USAEC Report ANL-5924, 1958.
[2] W.J. Mecham, J.D. Gabor, A.A. Jonke, Chem. Eng. Progr. Symp. Ser. 60 (47) (1964) 76.
[3] A.A. Jonke, Atomic Energy Rev. 3 (1965) 3.
[4] L.J. Anastasia, W.J. Mecham, I & EC Process Desi. Dev. 4 (1965) 338.
[5] T. Yahata, M. Iwasaki, J. Inorg. Nucl. Chem. 26 (1964) 1863.
[6] G. Vandenbussche, CEA-R 2859, 1966.
[7] M. Iwasaki, J. Nucl. Mater. 25 (1968) 216.
[8] J.C. Batty, R.E. Stickney, J. Chem. Phys. 51 (1969) 4475.
[9] B. Weber, A. Cassuto, Surf. Sci. 39 (1973) 83.
[10] A.J. Machiels, D.R. Olander, High Temp. Sci. 9 (1977) 3.
[11] H. Keil, P. Boczar, H.S. Park, Proceedings of the International Conference Tech. Expo. on Future Nuclear Systems, Global '93, Seattle, Washington, USA, 12–17 September 1993, p. 733.
[12] M.S. Yang, Y.W. Lee, K.K. Bae, S.H. Na, Proceedings of the International Conference Tech. Expo. on Future Nuclear Systems, Global '93, Seattle, Washington, USA, 12–17 September 1993, p. 740.
[13] Y. Kim, J. Min, K. Bae, M. Yang, J. Lee, H. Park, Proceedings of the International Conference on Future Nuclear Systems, Global '97, Yokohama, Japan, 5–10 October 1997, p. 1148.
[14] J.C. Martz, D.W. Hess, W.E. Anderson, Plasma Chem. Plasma Process. 10 (1990) 261.
[15] I.C. Plumb, K.R. Ryan, Plasma Chem. Plasma Process. 6 (1986) 205.
[16] D.L. Flamm, V.M. Donnelly, J.A. Mucha, J. Appl. Phys. 52 (1981) 3633.
[17] J.C. Martz, D.W. Hess, J.M. Haschke, J.W. Ward, B.F. Flamm, J. Nucl. Mater. 182 (1991) 277.
[18] W.C. Roman, Plasma Chem. Plasma Process. 1 (1981) 83.
[19] J. Fisher, M. Steindler, D. Steidl, ANL-6029 (1959).
[20] J.F. Moulder, W.F. Stickle, P.E. Sobol, K.D. Bomben, Handbook of XPS, Physical Electronics (1995).
[21] D.L. Flamm, in: D.M. Manos, D.L. Flamm (Eds.), Plasma Etching: An Introduction, Academic Press, New York, 1989, p. 91.